IEA SHC Task 64/SolarPACES Task IV – SubTask C: Assessment of uncertainties in simulation tools

Alan Pino[1], José Miguel Cardemil[2], Allan Starke[3], Leonardo Lemos[3], Vinicius Bonini[3], Ignacio Calderón[2], Ian Wolde[2], Carlos Felbol[4], Cristóbal Sarmiento[5] and Ignacio Arias[2]

[1] Department of Energy Engineering, University of Seville, Seville (Spain)
[2] Department of Mechanical and Metallurgical Engineering, Pontifical Catholic University of Chile, Santiago (Chile)
[3] Laboratory of Energy Conversion Engineering and Energy Technology (LEPTEN), Federal university of Santa Catarina, Florianopolis (Brazil)
[4] Center for Solar Energy Technologies (CSET) - Fraunhofer Chile Research, Santiago (Chile)
[5] School of Industrial Engineering, Diego Portales University, Santiago (Chile)

Abstract

Solar Heat for industrial processes has been a topic addressed in two previous Tasks of the Solar Heating and Cooling Program. Despite the huge advances achieved regarding the new knowledge, the number of SHIP installations worldwide is still far from the expectations. Task 64/IV aims to address part of the persisting entry barriers for SHIP systems. In the frame of Subtask C, it has been proposed to conduct a comparison campaign between the available simulation tools for yield assessment, allowing to identify the sources of differences between the simulation approaches. Therefore, four case studies based on the configuration of actual plants have been defined. In this study 12 different simulation tools were evaluated. Significant differences were observed between the tools' output, reaching deviations up to 49% for one configuration. The deviations also depend on the time resolution and the control volume considered for the analysis. This assessment could represent an important contribution for the industry towards an unification of the simulation approaches, reducing the perceived risk by the stakeholders.

Keywords: Solar Process Heat, Simulation Tools, Yield Assessment

1. Introduction

Solar thermal technologies have been recognized by several authors as a reliable option for delivering process heat to industrial processes (Farjana et al., 2018; Sharma et al., 2017). In addition, solar heat for industrial processes (SHIP) has been thoroughly studied in two Tasks of the Solar Heating and Cooling Program (SHC), Task 33 and Task 49. Nevertheless, despite the efforts and progress achieved in building new knowledge and reducing the entry barriers that solar thermal technologies face in the industrial heat market, the number of solar heat plants for industrial processes is less than 1,000 installations worldwide (Weiss and Spörk-Dür, 2020). In that context, a joint task between the SHC and SolarPACES programs started in 2020, Task 64/IV. It comprises a collaborative effort bringing together the experience from professionals, project developers, and scientists, aiming to address part of the entry barriers that hinder the further development of the market. The research questions addressed in the context of the Task are the standardization of integration schemes at the process and supply levels, as well as the combination with other efficient heat supply technologies such as combined heat and power plants, heat pumps, or power-to-heat. Furthermore, the identification of standardized industrial load profiles and the uncertainties associated with the simulation tools commonly used for yield assessment are also part of the challenges addressed in Task 64/IV.

Task 64/IV is divided into five subtasks: A, B, C, D, and E. Subtask C aims to address the lack of a standard simulation tool for SHIP installations. Currently, there are several simulation tools available, and the results delivered by each tool may differ significantly from each other. Therefore, Task 64/IV subtask C integrates the knowledge established in the previous Tasks 33 and 49, but taking the information according to the industry's "common language". Hence, bringing together the know-how and experience of several experts working with heat integration and heat management tools. In that context, the main objective of the subtask is to develop a deep analysis of the available simulation and monitoring tools for assessing the potential benefits of integrating solar heat into industrial processes, with known uncertainty sources. To achieve the objective, certain activities are carried out as the

© 2021. The Authors. Published by International Solar Energy Society
Selection and/or peer review under responsibility of Scientific Committee
doi:10.18086/swc.2021.29.02 Available at http://proceedings.ises.org

identification of the currently available simulation tools, and the classification of them according to their capabilities, simulation approaches, and software restrictions. Furthermore, four case studies have been defined in order to conduct equivalent simulations in different simulation tools, and to compare the results, identifying the differences and the impact on the main performance indicators. Accordingly, based on the results obtained, a guideline for developing yield assessment of SHIP plants will be developed, similar to the work carried out in SolarPACES Task I: Guideline for Bankable STE Yield Assessment (Hirsch, 2017).

To include different solar thermal technologies and industrial processes, the four case studies are based on actual SHIP plants, which are currently in operation. For low temperature, first a large plant comprised of flat-plate collectors on fixed mount is considered. The second case study considers a solar field of flat plate collectors mounted on 1-axis tracking systems, which represents a new trend in the SHIP industry. Furthermore, to assess medium temperature applications two technologies are considered: linear Fresnel collectors operating in a Direct Steam Generation (DSG) scheme, and parabolic trough collectors using water-glycol as heat transfer fluid (HTF).

The interaction among the participants of Subtask C is done through bi-monthly meetings. There is a core team responsible for preparing the parameters of the case studies' plants, receiving the results, and performing the comparison routines. The present study reports the main findings of the assessment, describes the work carried out during the first half of the Task work plan, and summarizes the activities executed and the main results obtained. In this regard, from the comparison it is observed that important differences in the solar yield are detected. For instance, differences for annual results are up to -20.3% for case 1, 49% for case 2, 84.2% for case 4, and 41.9% for case 5. For smaller timescales, such differences increase significantly. Furthermore, the main sources of the differences are seemingly obvious, however the methodology employed in this study allows to quantify the differences. The main of difference observed are the modeling of the control scheme, the modeling of the heat exchangers, time shift between the TMY data and the solar position, the modeling of internal flows, the assumptions about thermal capacitances, and the modeling of the thermal storage (from fully mixed to stratified).

2. Methodology

Since one of the main objectives of the Tasks is to pursue the contribution, interaction, and discussion from several experts in the field, the authors of this study have been in continuous interaction with the Subtask C participants, who belong to different institutions around the globe. The authors have been working as a core team which leads and manages Subtask C activities, mainly providing the information to other participants, receiving the information, performing the analysis, and presenting the results.

For the specific activities that are covered in this study, i.e., the assessment of uncertainties in simulation tools, the highlighted section of the flowchart presented in **Fig.1** has been followed. First, a case study is selected. This means specifying a solar thermal installation currently in operation or being built. The main requisite is to have enough detailed information regarding the design (either public or private) to model the system in a simulation tool for yield assessment. For instance, the information should at least include the manufacturer and model of the collector employed (or performance curve), size, orientation and slope of the solar field, size, geometry and insulation characteristics of the thermal storage (if existing), details of heat exchangers, load profile (mass flow and temperature), and finally the control philosophy (including pump features).

In a second stage, all the technical information is compiled in a unique file (spreadsheet) that is distributed to the simulation specialist, who develops their simulation model in their preferred simulation tool. In addition to the technical features, the meteorological information (TMY format) is supplied along with a template spreadsheet to report the simulation results.

Once the results from the different analysts have been received, they are compared according to the metrics selected for this purpose, as detailed in Section 2.2. It is necessary to select one of the tools as a reference tool, which do not need to be the same for all the case studies. The comparisons are made considering different control volumes of the plant, according to the stages of energy flow, i.e., in the solar field, in thermal storage, and in the load to process. To assess the differences in the results reported, four time resolutions are considered for the comparison routine: hourly, daily, monthly, and annual values.

As a result of the comparison, the main sources of deviations between results from each simulation tool and the results of the reference tool are identified and quantified in a preliminary manner, according to the metrics employed. To improve qualitative analysis, bilateral meetings were held between the core team and each of the analysts during the first semester of 2021. The objective of these meetings is to understand the assumptions that the analysts have

considered, differentiating when they are due to lack of information about the system design, from the intrinsic limitations of modeling approach, and solution strategy of the software employed.

Feedback to the analysts is also given, based on the comparison of results. The aim is to enhance their models by improving the assumptions made due to lack of information, but not to alter their results to be closer to the reference tool. Hence, a second round of simulation is carried out, allowing to conduct an equivalent analysis and identification of sources of differences.

The final steps of the complete assessment, include the last three stages of the flow chart in Fig. 1, not presented in this study. Sources of differences are categorized according to the impact on the final energy yield. Since different software and different analysts might increase the bias and uncertainties in the analysis, a parametric analysis is performed varying the parameters associated with the sources of differences previously identified. This parametric analysis is carried out using one single reference tool and by the same analyst, with the aim of isolating (or reducing) the impact of the human factor. Finally, the final impact assessment and sources of differences are established.

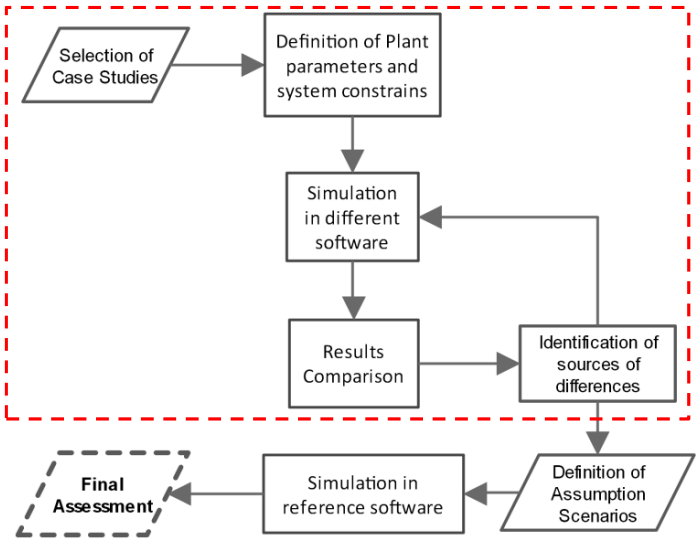

Fig. 1: Flowchart of methodology utilized to identify the sources of differences in the results of energy yield performed by different analysts employing different simulation tools (software).

2.1. Definition of case studies

In order to cover a broader range of temperatures and applications, four case studies have been analyzed employing the methodology mentioned above. They are numbered 1, 2, 4, and 5 because the analysis of case study 3 is pending. Since this is an ongoing activity, the progress of the analysis is different for the 4 cases.

The information presented in this section summarize the main plant parameters and the operation scheme for each case study. However, there is more information available, and it was supplied to the analysts to build the simulation models, especially regarding hourly load profile, efficiency of solar field, geometry and insulation of the storage, effectiveness of the HXs, pumps mass flow and efficiency, control philosophy, among others.

Case study 1: flat plate collectors (FPC) to supply hot water to a copper mining process. The system supplies heat to a copper electrowinning plant located in the Atacama Desert, Chile (lat. 23.45° S, long. 68.81° W, annual GHI 2,631 kWh/m^2). The plant is comprised by a 39,300 m^2 solar field of fixed flat plate collectors, with a thermal storage tank of 4,300 m^3. The coupling scheme is considered through two heat exchangers, one between the solar field and the thermal storage tank, and the other between the storage and the load. A simplified layout for the plant is depicted in **Fig 2**. The HTF considered in the solar field is a water-glycol mixture (33% glycol), while the energy storage uses demineralized water. In addition, the working fluid of the process is water, where the set point temperature of the process is 70 °C and the return temperature is 40 °C. The annual heat demand is 94,171 MWh with a constant load profile (24/7) (Quiñones et al., 2020).

The solar field circuit is controlled by a differential temperature controller, which activates the circulation pump when the solar field outlet temperature is higher than the temperature at the bottom of the storage tank plus a dead band of 10 °C. In addition, a lower dead band of 2 °C is considered to turn the pump off. The temperature at the top of the tank is monitored for safety purposes to avoid boiling, so it deactivates the pump when it reaches 100 °C. On the thermal storage side and load circuit, since there is a fixed mass flow pump, the HX that supplies the load has a

bypass to avoid heating the water to the process over 82.6 °C.

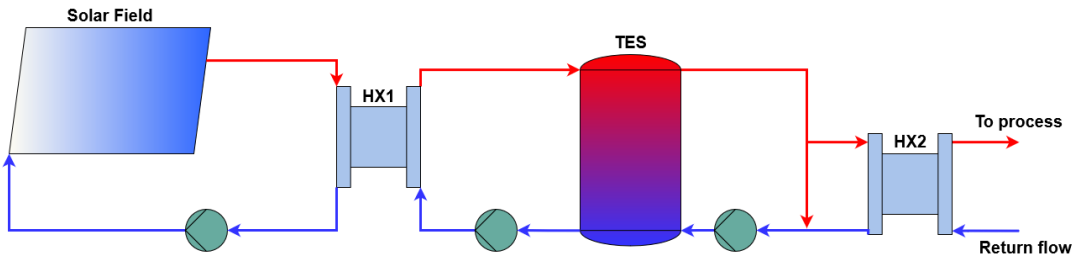

Fig. 2. System diagram of case study 1, flat plate collectors to supply hot water to a copper mining process.

Case study 2: 1-axis tracking flat plate collectors (FPC) to supply hot water to a paper mill process. The system supplies hot water as a preheating stage to a feed a gas boiler coupled to a paper mill factory located in Dordogne, France. The total gross collector area is 4,212 m^2, and the storage tank volume is 457 m^3. The solar collectors are installed on a 1-axis tracking system that allows to maximize the heat production, and even reduce it, if necessary, by defocusing. The primary circuit (solar field) employs a water-glycol mixture as HTF. The make-up water to be heated is continuously provided by the demineralized unit of the paper mill. Both primary and secondary circuits employ variable-speed pumps controlled to maximize solar field output. The layout is depicted in Fig. 3. There is no fixed set-point temperature for the water delivered by the solar plant to the process. However, the maximum feedwater temperature to the boiler is 80 °C. The temperature setpoint to be reached at the collector outlet evolves throughout the year from 30 ° C (in winter) to 90 ° C (in summer), in order to maximize the production of solar heat.

The control strategy is the following. (a) when a threshold of irradiance on the surface of the collector is reached, the pump on the solar field circuit is turned on. At this point there is recirculation only on the solar field until the set temperature at the solar field outlet is reached. (b) When the set temperature is achieved, the flow goes through the heat exchanger and the pump of the secondary circuit is turned on. The pump operates in a closed circuit between the HX and the thermal storage. Both pumps are of variable speed and controlled to maximize the energy transfer at the HX, taking into account the set temperature at the solar field outlet. (c) When the process demands heat, water from the top of the thermal storage is employed. At the same time, cold water is pumped into the bottom of the tank to keep the volume constant.

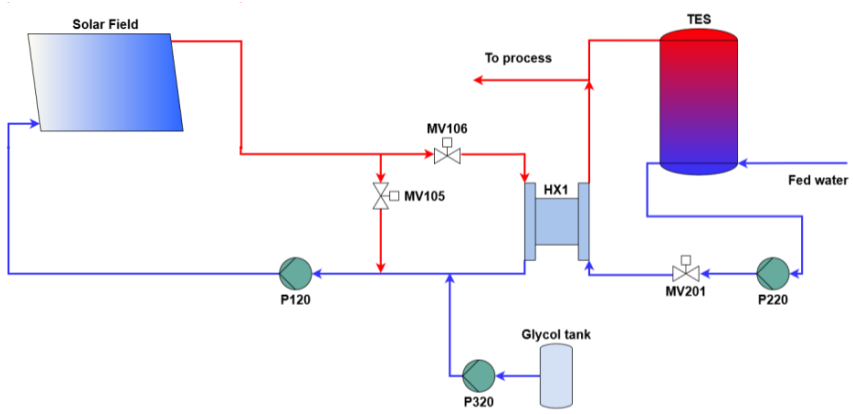

Fig. 3. System diagram of case study 2, 1-axis tracking flat plate collectors to supply hot water to a paper mill process.

Case study 3: Pending. Case study on-hold while waiting for additional information to perform the uncertainty analysis.

Case study 4: linear Fresnel collector (LFR) for direct steam generation (DSG). The system analyzed corresponds to a system configured by the company Solatom, which consists of Fresnel FTL20 solar collectors. FLT20 modules are pre-assembled and packed at the factory, and then transported ready to be installed. Each module has a thermal power of 14.5 kW_{th} and is suitable for installation on rooftops. The system operates in the direct steam generation (DSG) scheme, and located in Seville (Spain), integrated in recirculation mode with a steam drum. The water-steam mixture generated by the solar field feeds the steam-drum, where the saturated liquid is fed back to the collector loop by the circulation loop. In case of sufficient pressure in the steam drum, the saturated steam is fed into

the conventional steam circuit (load). The total area of the reflective surface is 1900.8 m^2 and is structured in 6 loops with 12 modules each (the area of a single collector is 26.4 m^2). The layout of the plant is depicted in Fig. 4. The annual heat demand is 4,858 MWh. The typical daily load profile is presented by de Santos López (2021). Saturated steam is provided to the process at 6 bar (158.5 °C), with the condensates returning at 70 °C. The steam demand is supplied by the solar system with the aid of a auxiliar natural gas boiler installed in parallel (not considered in the simulations) for low irradiation periods.

The control system is configured to maintain the operation conditions of the plant following these settings: (a) start-up, boiler feed water recirculates in the field steam drum loop until pressure reaches the requirements; (b) normal operation, the steam from the steam drum is delivered to the steam line; (c) shutdown, decreases the mass flow rate as irradiation decreases, reaching a minimal value. The following control philosophy applies: if the nominal conditions could be met, go to recirculation; if the minimal flow rate is larger than the demand, go to recirculation; for operation on nighttime and/or low solar resource: "minimum flow rate in single collector loop".

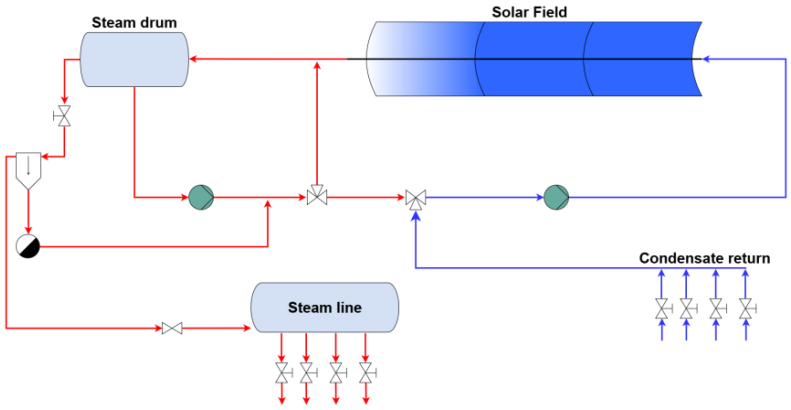

Fig. 4. System diagram of case study 4, linear Fresnel collector (LFR) for direct steam generation.

Case study 5: parabolic trough collectors to supply hot water to a dairy plant. The system consists of a PTC field installed on the roof of a dairy factory, coupled to an existing system located in Saignelégier, Switzerland. A total of 17 PTC rows are installed, where one collector per row is implemented. The solar field operates with a water-glycol mixture, which is heated to a design temperature of 110°C. The HTF is sent to a heat exchanger with a nominal heat transfer rate of 350 kW. The thermal energy from the collectors is used to heat the pressurized water of the process up to a design temperature of 105°C. The hot water flows to the boiler and storage system of the plant, from where it is distributed to the processes involved in the dairy production. A simplified layout of the plant is depicted in Fig. 5.

The control strategy considered for the system is the following. When heat is required, and the direct solar radiation exceeds a predefined threshold (250 W/m^2), the collectors are automatically turned towards the Sun and the pump starts to circulate. The flow rate in the solar circuit is controlled by a frequency converter to maintain the set temperature (between 110 and 120 °C). If this temperature exceeds the maximum allowed value, the sensor defocuses automatically. High-temperature shut-off happens only if high flow is detected. A shut down occurs when the direct solar irradiance is lower than 100 W/m^2.

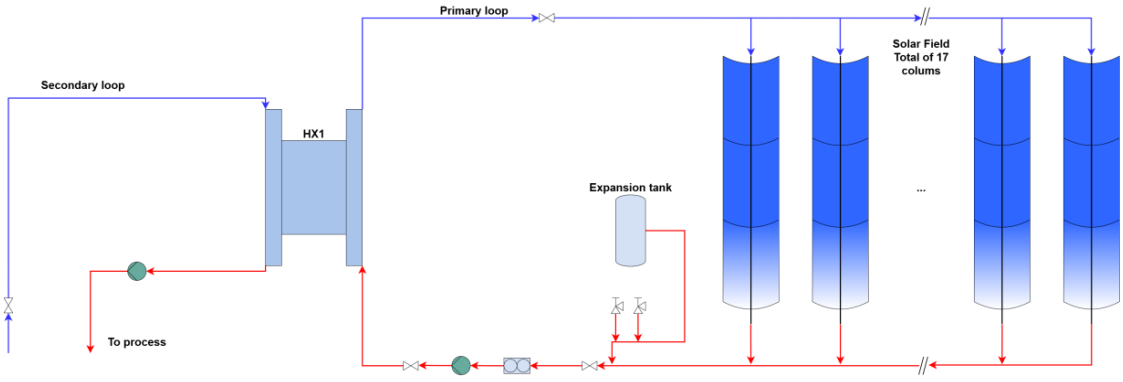

Fig. 5. System diagram of case study 5, parabolic trough collectors to supply hot water to a dairy process.

2.2. Metrics for the assessment of differences/deviations

In order to configure a flexible tool for comparing the different simulation results of the cases under study, a unified open-source script for the treatment of hourly, daily, monthly, and annual time scales was programmed using Python; thus, different open-source packages were used. In this way, Matplotlib, Pandas, Numpy, and skill_metrics packages were used (Harris et al., 2020; Hunter, 2007; McKinney, 2010). These packages are useful both for data visualization and generation of figures for all time scales and for reading, processing, post-processing, and calculating statistical comparison parameters. In addition to that, Glob and Os packages were used to manipulate file paths. In this way, normalized root mean square (nRMSE), normalized mean bias error (nMBE), relative difference, the root mean square difference of the pattern (RMSD), Pearson correlation coefficient (R), and the standard deviation (σ) were calculated as established statistical comparison metrics. Nevertheless, at the hourly level, RMSD, R and σ were correlated within a Tylor diagram to visualize their deviation from the reference case. The pattern root mean square difference is presented in eq. 1.

$$RMSD = \sqrt{RMSE^2 + RMSE_{ref}^2 - 2 \cdot RMSE \cdot RMSE_{ref} \cdot R} \qquad \text{(eq. 1)}$$

where $RMSE$ is the root-mean-square of the tool to compare with the reference, $RMSE_{ref}$ is a root-mean-square of the reference, and R is the Pearson correlation between test and reference.

Furthermore, the Dynamic Time Warping (DTW) algorithm was employed for analyzing hourly results as a method to size and compare the time series difference between the results reported by the reference and the other tools, with respect to certain parameters. Currently, DTW is used in similarity tests, also for clustering and machine learning algorithms (Zhang et al., 2021). Thus, a typical code of the DTW algorithms is presented in the Tab. 1.

Tab. 1: Algorithm for computing the Dynamic Time Warping

DTW algorithms
Input: Q = $\{q_1, q_2, \dots, q_m\}$ and $C = \{c_1, c_2, \dots, c_\pi\}$ // the two time-series Output: The optimal warping path; The distance of Q and C.
Initialize: DTW(1,1) = $d_{1,1}$ For i=1:n For j=1:m D1= $d_{i,j} + DTW(i-1, j)$ D2= $d_{i,j} + DTW(i-1, j-1)$ D3= $d_{i,j} + DTW(i, j-1)$ DTW= min(D1,D2,D3); The optimal $path_{i,j}$ = min_index($(i-1, j), (i-1, j-1), (i, j-1)$) End End

Therefore, the purpose of using the DTW in this study is to quantify phase and amplitude errors, as well as to contrast the similarity between the temporal sequences with respect to the reference, and the sensitivity and relationship of DTW with other statistical established metrics (Gaspar et al., 2017). The main advantage of DTW over other established statistical metrics, such as RMSE and MBE, is related to the reliable alignment between the reference and test patterns. However, one of the main disadvantages of using DTW is related to a more robust computational effort to find the optimal alignment path in time (Brown and Rabiner, 2005).

Although the RMSE is more intuitive, it reports on the average size of the forecast errors regardless of their sign. Therefore, the biggest advantage of the RMSE is related to the measurement of uncertainty in the calculation of forecasts. However, two important disadvantages are observed; first, it is an absolute uncertainty metric that makes a comparison through highly variable time series, and that it is influenced by outliers. Therefore, it is not used to see the dynamic evolution of the series (Brown and Rabiner, 2005; Gaspar et al., 2017; Li et al., 2020) .

2.3. Simulation tools employed

There was no restricting criterion for selecting the simulation tools. Any participant of the Subtask C that was trained in a simulation tool and willing to contribute was welcome. Hence, it was possible to include in the study licensed software, open-source software, and in-house developed software. The participants/analysts also delivered a brief simulation log together with the results where the main assumptions and limitations of the software for a specific component were indicated, e.g., if the software cannot model the thermal storage losses, a penalizing factor is added by the analyst to the energy yield. Tab. 2 summarizes the tools/software employed for each case study.

Tab. 2. List of tools/software employed for the different case studies.

Case study 1	CEA model, Greenius, SHIP2FAIR tool, SHIPcal, System Advisor Model (SAM) TRNSYS - TESS library, TRNSYS - basic library.
Case study 2	NewHeat tool, Polysun, SHIP2FAIR tool, TRNSYS (3 simulations models employing different libraries)
Case study 3	Status: pending
Case study 4	Greenius, SAM, Scilab, SHIP2FAIR tool, SHIPcal, TRNSYS (4 simulation models employing different libraries)
Case study 5	Greenius, Polysun, TRNSYS

3. Results and Discussion

In order to compare the simulation results from the different simulation tools and cases, a reference tool is selected for each case. The "deviations" of the results between the different tools and the reference are calculated using the metrics described in Section 2.2. The reference tool is named Tool 0 for all case studies. When available, Tool 0 corresponds to the tool employed by the project developer during the design stage of the SHIP plant. The tools have been purposely randomly numbered for the benchmark analysis to avoid the unintended message of ranking the tools.

Case study 1. The annual and monthly energy delivered to the load for case study 1 is presented in Fig. 6. It can be observed that in the annual analysis tools 1 and 2 overestimate the energy yield, and tools 3, 4, 5, and 6 underestimate it. There are no large differences in the output (up to 6.45%), with the exception of tool 5 which underestimate the energy to the load by 20.3% when compared to the reference. The monthly results indicate a similar behavior in the shape of curves, but certain values highly disagree. For instance, tool 5 delivers 35% less energy to the load compared to the reference in June.

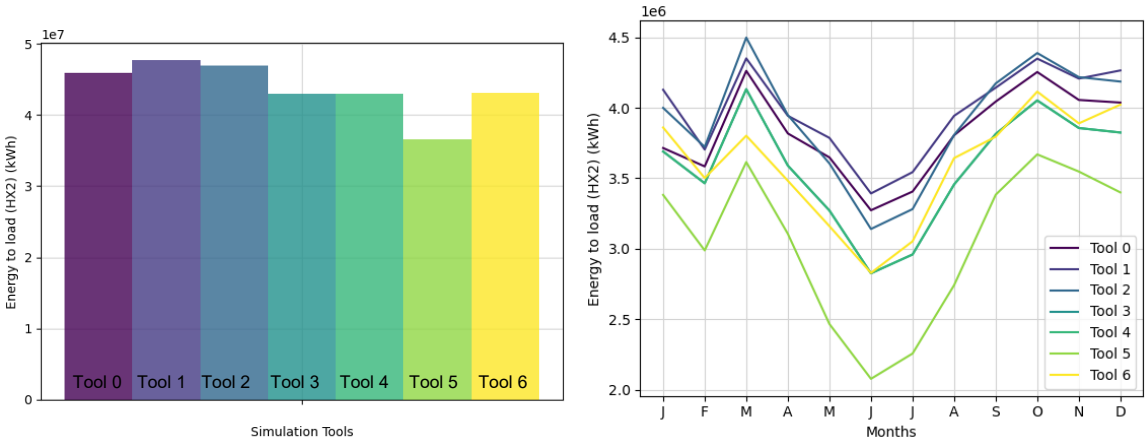

Fig. 6. Annual and monthly figures of energy yield to the load obtained by the different tools for case 1.

The Fig. 7 (left) presents a daily comparison of the different DTW profiles between the reference tool and the other tools used in the analysis. The comparison is shown in terms of the absorbed solar radiation (q_{in}), heat to the TES (q_{hx1}), and the heat to the load (q_{hx2}). The first plot shows a low value for the DTW for all tools, except for tool 6 (yellow lines), suggesting that a different approach for the weather input is used for this simulation. Its effect is also

observed in the other control volumes. For the rest of the tools, it is noticeable that the indicator increases its value as it goes through the control volumes in the direction of the energy flow (from irradiation to load). Therefore, it is observed that the different assumptions and simulation approaches may contribute to the overall error as the simulation model increases in number of components. On the right plot of Fig. 7, certain days are selected to present the hourly evolution. It can also be observed that tool 6 has a mismatch in the TMY data compared to the rest. In addition, for the heat supplied to the load (q_{hx2}) it is observed the effect of the thermal storage modeling. The periods where the curve saturates to a constant value are explained by assuming an approach with a single-node tank. Thus, it charges and discharges at continuous energy rates between the set and the minimum temperatures. On the other hand, the periods where the curve increases and decreases with a steady slope means that the tank is stratified. Hence, the tank can deliver lower energy rates due to a lower outlet temperature.

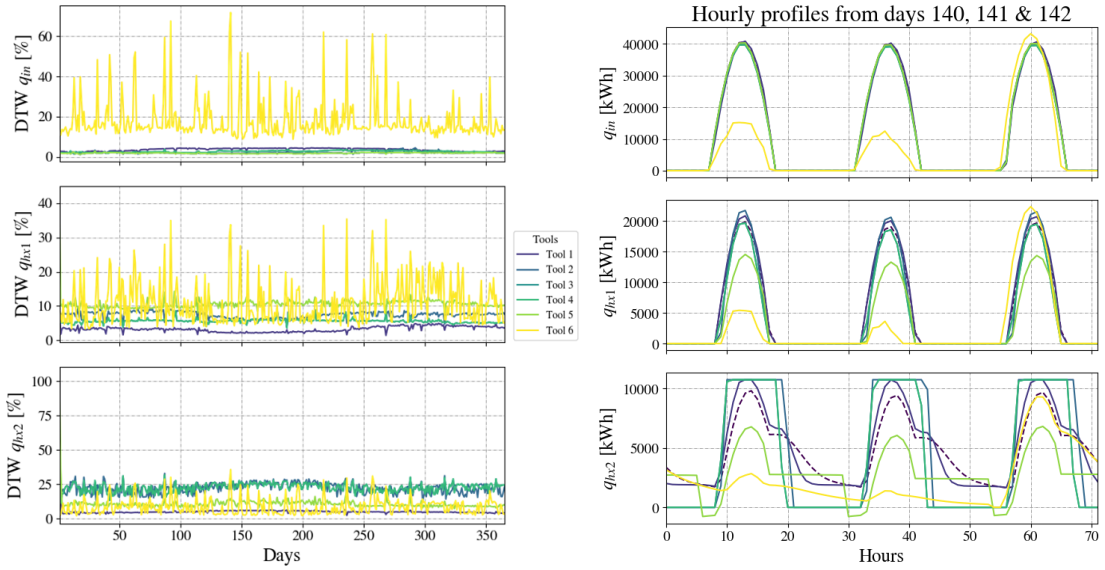

Fig. 7. Dynamic Time Warping (DTW) on daily timescale (left) and hourly profiles for selected days (right) for Case 1.

Case study 2. Similarly to case study 1, the annual and monthly energy yield for case study 2 are presented in Fig. 8. In this case the results reported by tools 1 and 4 are extremely similar to the reference tool, both in annual and monthly time resolution, with an annual difference under 1%. On the other hand, results reported by tools 2, 3 and 5 underestimate annual and monthly values of energy delivered to the load. These differences are -8.3% for Tool 3, -27% for Tool 5 and –49% for Tool 2. Monthly results agree with the annual values. However, there is a trend during certain months of the year, where the difference between some tools and the reference tool is higher, i.e., tools 2, 3, and 5. The difference increases during summer months with higher solar resource availability. Conversely, during winter months, such as December or January, there are smaller absolute differences with the reference tool.

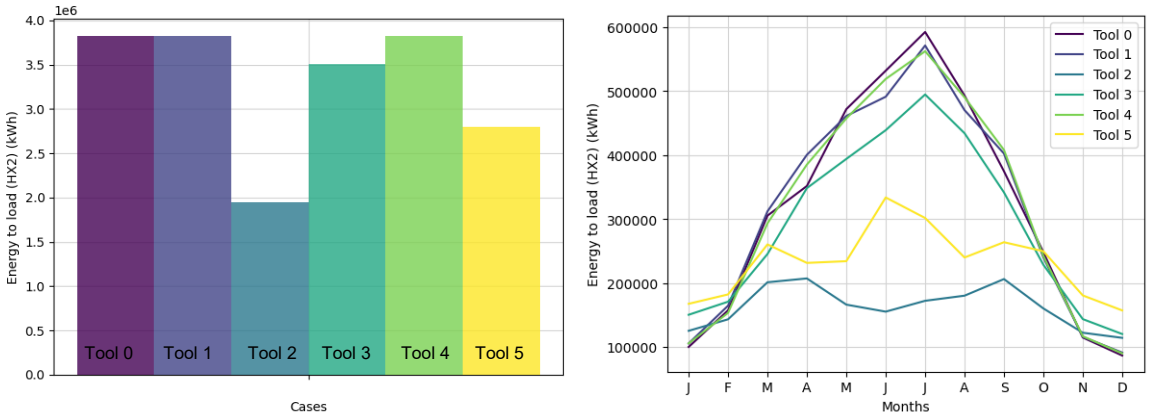

Fig. 8. Annual and monthly figures of energy yield to the load obtained by the different tools for case 2.

Case study 4. The annual and monthly energy yield to the load for case study 4 are presented in Fig. 9. In this case, the results reported by tools 1, 3, 5, 6, and 7 are similar to the reference tool, with an annual deviation under 10%. In addition, the results reported by tools 4 and 8 underestimate annual energy delivered to the load, with an overall

difference of -19.5% and –17.7%, respectively. For monthly values, tool 8 underestimates in summer (April to September). Moreover, although Tool 4 is close to the reference in July and August, it consistently underestimates the energy yield from November to June, and overestimates in September and October. Furthermore, Tool 2 presents the largest difference with the reference tool. It presents significant higher values, for both annual and monthly results, overestimating in 84.2% the annual value of the reference.

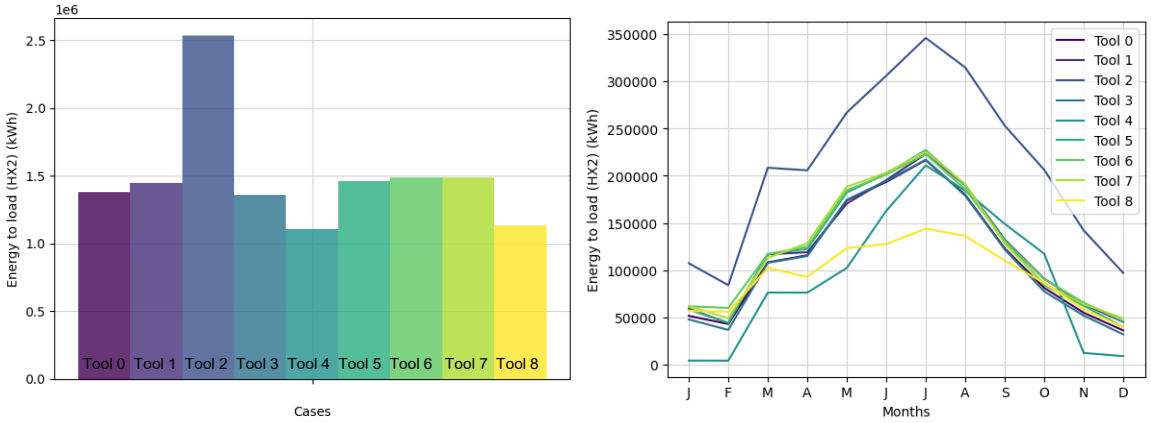

Fig. 9. Annual and monthly figures of energy yield to the load obtained by the different tools for case 4.

Case study 5. For this case study only 3 sets of results have been collected (depicted in Tab. 2). Therefore, the comparison analysis has not been concluded. However, Fig. 9 present the annual and monthly energy yield. As preliminary observations, for annual values Tool 1 underestimates the energy supplied to the load (-11%), whilst Tool 2 greatly overestimates it (41.9%). When the monthly figures are observed, it is noticeable that Tool 1 underestimate the energy yield in winter months but overestimate it in summer. Tool 2 has an odd behavior with high peaks in March and June, which leads to overestimate the overall energy yield.

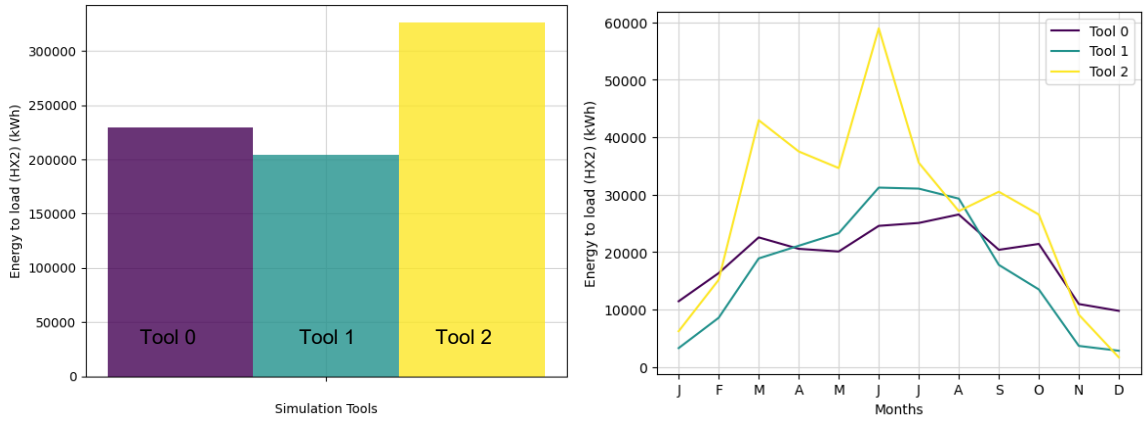

Fig. 10. Annual and monthly figures of energy yield to the load obtained by the different tools for case 5.

To summarize the results from the comparison analysis, Tab. 3 presents the differences observed in the total energy yield to the load for the 4 case studies, when compared to each reference tool. The normalized RMSE is presented for the monthly values, whilst the percentual difference is presented for the annual values.

In addition, Tab. 4 presents the values for the DTW from the hourly comparison normalized by the annual load. The table is separated by case study and tool. For each case study different control volumes are analyzed, i.e. the supplied energy is calculated at different stages of the energy flow to the load. For example, for case study 1 three control volumes are considered: (a) solar field, where the incident radiation on the collector's surface is calculated; (b) heat exchanger between solar field and storage tank, where the energy transferred to the tank is calculated; and (c) heat exchanger between the storage tank and the load, where the total energy yield to the load is calculated. The DTW represents a cumulative distance from the reference, hence lower DTW are desirables. It can be observed that DTW increases when the control volume is closer to the load (maximum values). It means that the deviations of the simulation results at different components impacts the next component on the direction of the energy flow to the load. Frequently, the monthly and annual values hide certain differences when integrating the values over the period,

as positive and negative deviations are compensated.

Tab. 3. Summary of the differences observed from the simulations in the four case studies.

Case	Value	Time scale	Metric	tool 1	tool 2	tool 3	tool 4	tool 5	tool 6	tool 7	tool 8
1	Energy to load	Monthly	nRMSE	0.05	0.04	0.07	0.07	0.21	0.08	-	-
		Annual	% diff.	4.03	2.32	-6.5	-6.5	-20.3	-6	-	-
2	Energy to load	Monthly	nRMSE	0.07	0.69	0.18	0.06	0.49	-	-	-
		Annual	% diff.	-0.05	-49	-8.3	-0.12	-26.8	-	-	-
4	Energy to load	Monthly	nRMSE	0.06	0.88	0.02	0.33	0.07	0.09	0.08	0.31
		Annual	% diff.	5.30	84.2	-1.6	-19.5	6.1	8.3	8	-17.7
5	Energy to load	Monthly	nRMSE	0.31	0.74	-	-	-	-	-	-
		Annual	% diff.	-11	41.9	-	-	-	-	-	-

Tab. 4. Summary of the comparison results in terms of the DTW.

Case	Parameter	Normalized DTW %	Tool 1	Tool 2	Tool 3	Tool 4	Tool 5	Tool 6	Tool 7	Tool 8
1	Incident radiation	min	1.34	1.07	1.45	1.45	1.12	8.73	-	-
		max	4.41	4.42	3.61	3.61	2.79	71.83	-	-
	Energy to TES	min	1.44	3.69	3.63	3.63	7.73	3.38	-	-
		max	9.25	9.24	8.84	8.84	42.79	32.34	-	-
	Energy to load	min	2.51	13.12	11.54	11.54	7.44	1.83	-	-
		max	56.03	32.99	31.83	31.83	104.91	35.78	-	-
2	Incident radiation	min	0.30	0.53	0.29	0.24	0.29	-	-	-
		max	7.61	33.82	11.21	10.59	26.95	-	-	-
	Energy to TES	min	0.00	0.07	0	0	4.21 e-05	-	-	-
		max	9.91	37.46	13.46	17.21	20.39	-	-	-
	Energy to load	min	0.04	0.07	0.79	0.38	0.57	-	-	-
		max	21.0	65.47	38.64	20.24	34.76	-	-	-
4	Incident radiation	min	8.02e-8	5.33e-17	4.56e-4	2.46e-16	0.29	NA	0	0
		max	0.014	5.39	0.004	2.13	16.39	NA	1.45e-14	1.45e-14
	Energy to load	min	0	0.42	0	0.23	3.10e-05	NA	0	0
		max	5.56	34.98	19.72	18.67	18.78	NA	15.06	18.99
5	Incident radiation	min	2.21	3.15	-	-	-	-	-	-
		max	14.27	85.93	-	-	-	-	-	-
	Energy to load	min	0.19	0.19	-	-	-	-	-	-
		max	47.46	138.65	-	-	-	-	-	-

Notes: - For case 1, tool 6 presents a high DTW value for the incident radiation due to initialization of the operation variation.
- For case 4, tool 6 did not report hourly results.

From the analysis of the DTW results and the direct comparison of hourly curves, the main sources of difference are identified. For instance, time delays or shifting between the reference and the tools are due to shift in the sun position, consideration or not of the components' heat capacitance, and modeling of the control philosophy. In addition, certain absolute differences of energy flow are due to modeling of the thermal storage (stratified, hot and cold tanks, or fully mixed), modeling of the heat exchangers, and considering the thermal losses of piping.

4. Conclusions

The present study describes the initial results obtained by the comparison campaign of simulation tools employed for yield assessment of SHIP plants. The motivation of the study was associated to the large number of simulation

tools available in the market, lacking a standardized one. Moreover, it was noticed that most of the project developers employ their in-house developed tools. The main advantage observed regarding the different tools is the broad range of system configurations that can be modeled, and the high flexibility that most of the tools present. However, certain tools have been developed to model specific systems and do not perform appropriately for technologies different from the original, e.g., a software developed for tracking-concentrating systems employed for non-concentrating collectors. Therefore, to ensure that the results obtained from the yield assessments can be directly compared it is necessary to develop a guideline for performance comparisons of SHIP simulations, like the work carried out for CSP systems.

The activities performed within the Subtask C have been highly time-consuming. Nevertheless, the participation of more than 30 experts and analysts from different international institutions enriches the feedback obtained for the analysis and increases the opportunity of understanding several different simulation approaches. Although the results of the comparisons seem to be evident and expected, several deviations observed were not directly linked to assumptions that might be trivial. For instance, the meteorological data is commonly an input for the simulations (usually in TMY format); however, the software's internal radiation processor can incorrectly use a different time stamp than the one from the meteorological file.

Regarding the comparison of the results obtained from the simulation tools, several anomalous behaviors are noticed. First, for annual values certain cases present large deviations from the reference tools (up to -20.3% for case study 1, 49% for case study 2, 84.2% for case study 4, and 41.9% for case study 5). Since the annual energy yield hides several short-term effects, e.g., seasonal variations, the differences observed are too high to assume that the SHIP plants performance is correctly estimated. Hence, the risk for the financial assessment increases, and consequently, the competitiveness of solar thermal technologies against non-renewable is highly reduced.

The assessment described in the present article could initially aid unifying criteria for modeling assumptions and defining simulation approaches. With further analysis it also aid in reducing the "risk" perceived by the financial industry and facilitating the interaction with the potential consumers. This is an ongoing study. Since relevant deviations in the results were observed at this stage, that only considers simulations, actual operation data will be employed in a second stage of the project. The operation data will be employed as the reference to assess the differences in the plant performance estimated by the simulation tools. Finally, the key findings of these comparisons will serve as input to create guidelines for implementing computational tools to assess and monitor the performance of SHIP systems, which are part of the deliverables of Subtask C.

5. Acknowledgments

The authors gratefully acknowledge all the participants of Task 64/IV subtask C that have contributed with the simulations, in particular to J. Dersch and J. Labairu (DLR), R. Albert (CEA), A. Gonnelle (NewHeat), M. Nájera (CIMAV), G. de Santos (KTH), A. Cazorla (UPV), D. Theiler (SPF), E. Burin (UFPR), P. Kurup (NREL), M. Frasquet (SOLATOM).

The authors also acknowledge the financial support from ANID/FONDAP 15110019 "Solar Energy Research Center" - SERC-Chile and the project ANID/FONDECYT/1191705. A. Pino acknowledges financial support from ANID PFCHA/DOCTORADO BECAS CHILE/2017. I. Arias acknowledges the funding from ANID PFCHA/Doctorado Nacional 2021-21210053. Finally, this study was partially funded by the Coordenação de Aperfeiçoamento de Pessoal de Nível Superior – Brasil (CAPES) – Finance Code 001, via a scholarship to Leonardo Freire Lacerda Lemos.

6. References

Brown, M., Rabiner, L., 2005. Dynamic time warping for isolated word recognition based on ordered graph searching techniques, in: ICASSP '82. IEEE International Conference on Acoustics, Speech, and Signal Processing. Presented at the IEEE International Conference on Acoustics, Speech, and Signal Processing, Institute of Electrical and Electronics Engineers. https://doi.org/10.1109/icassp.1982.1171695

de Santos López, G., 2021. Techno-economic Analysis and Market Potential Study of Solar Heat in Industrial Processes (Master of Science). KTH Royal Institute of Technology.

Farjana, S.H., Huda, N., Mahmud, M.A.P., Saidur, R., 2018. Solar process heat in industrial systems – A global review. Renewable Sustainable Energy Rev. 82, 2270–2286. https://doi.org/10.1016/j.rser.2017.08.065

Gaspar, M., Welke, B., Seehaus, F., Hurschler, C., Schwarze, M., 2017. Dynamic Time Warping compared to established methods for validation of musculoskeletal models. J. Biomech. 55, 156–161. https://doi.org/10.1016/j.jbiomech.2017.02.025

Harris, C.R., Millman, K.J., van der Walt, S.J., Gommers, R., Virtanen, P., Cournapeau, D., Wieser, E., Taylor, J., Berg, S., Smith, N.J., Kern, R., Picus, M., Hoyer, S., van Kerkwijk, M.H., Brett, M., Haldane, A., Del Río, J.F., Wiebe, M., Peterson, P., Gérard-Marchant, P., Sheppard, K., Reddy, T., Weckesser, W., Abbasi, H., Gohlke, C., Oliphant, T.E., 2020. Array programming with NumPy. Nature 585, 357–362. https://doi.org/10.1038/s41586-020-2649-2

Hirsch, T., 2017. Guideline for Bankable STE Yield Assessment. SolarPACES.

Hunter, J.D., 2007. Matplotlib: A 2D Graphics Environment. Comput. Sci. Eng. 9, 90–95. https://doi.org/10.1109/mcse.2007.55

Li, H., Liu, J., Yang, Z., Liu, R.W., Wu, K., Wan, Y., 2020. Adaptively constrained dynamic time warping for time series classification and clustering. Inf. Sci. 534, 97–116. https://doi.org/10.1016/j.ins.2020.04.009

McKinney, W., 2010. Data Structures for Statistical Computing in Python, in: Proceedings of the 9th Python in Science Conference. Presented at the Python in Science Conference, SciPy. https://doi.org/10.25080/majora-92bf1922-00a

Quiñones, G., Felbol, C., Valenzuela, C., Cardemil, J.M., Escobar, R.A., 2020. Analyzing the potential for solar thermal energy utilization in the Chilean copper mining industry. Solar Energy 197, 292–310. https://doi.org/10.1016/j.solener.2020.01.009

Sharma, A.K., Sharma, C., Mullick, S.C., Kandpal, T.C., 2017. Solar industrial process heating: A review. Renewable Sustainable Energy Rev. 78, 124–137. https://doi.org/10.1016/j.rser.2017.04.079

Weiss, W., Spörk-Dür, M., 2020. Solar-Heat-Worldwide 2020. IEA - Solar Heating and Cooling Programme.

Zhang, J., Johnstone, M., Le, V., Khan, B., Anwar Hosen, M., Creighton, D., Carney, J., Wilson, A., Lynch, M., 2021. Dynamic time warp-based clustering: Application of machine learning algorithms to simulation input modelling. Expert Syst. Appl. 186, 115684. https://doi.org/10.1016/j.eswa.2021.115684